

UNVEILING CROSS MODALITY BIAS IN VISUAL QUESTION ANSWERING: A CAUSAL VIEW WITH POSSIBLE WORLDS VQA

A PREPRINT

Ali Vosoughi³, Shijian Deng², Songyang Zhang¹, Yapeng Tian², Chenliang Xu¹, Jiebo Luo^{1,3}

¹Dept. of Comp. Sci., University of Rochester, Rochester, NY 14620

²Dept. of Comp. Sci., University of Texas Dallas, Dallas, TX 12345

³Dept. of ECE, University of Rochester, Rochester, NY 14620

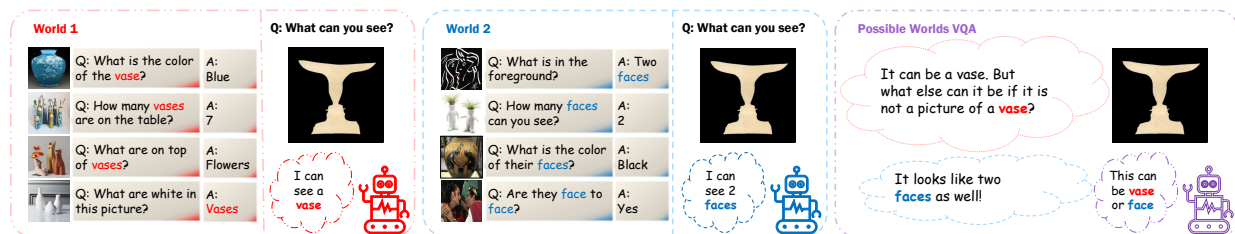


Figure 1: Visual cognition of annotators is related to the language Lupyan et al. [2020], which in turn influences the choice of questions and answers to those questions. A well-known example of Rubin’s vase shown in this figure Rubin [1915] is to illustrate how memory and experience can affect the perception of the annotator.

ABSTRACT

To increase the generalization capability of VQA systems, many recent studies have tried to de-bias spurious language or vision associations that shortcut the question or image to the answer. Despite these efforts, the literature fails to address the confounding effect of vision and language simultaneously. As a result, when they reduce bias learned from one modality, they usually increase bias from the other. In this paper, we first model a confounding effect that causes language and vision bias simultaneously, then propose a counterfactual inference to remove the influence of this effect. The model trained in this strategy can concurrently and efficiently reduce vision and language bias. To the best of our knowledge, this is the first work to reduce biases resulting from confounding effects of vision and language in VQA, leveraging causal explain-away relations. We accompany our method with an explain-away strategy, pushing the accuracy of the questions with numerical answers results compared to existing methods that have been an open problem. The proposed method outperforms the state-of-the-art methods in VQA-CP v2 datasets.

*Equal contribution

1 Introduction

Visual Question Answering (VQA) systems are one of the most fundamental building blocks at the intersection of vision and language Zellers et al. [2019], Niu et al. [2021], Kolling et al. [2022]. VQA systems use linguistic and visual information to obtain correct and robust answers to given questions from an image. Despite the efforts, regrettably, most VQA systems shortcut directly from the vision or language to an answer Niu and Zhang [2021], Cadene et al. [2019a,b]. This shortcut is known as vision or language bias and has been well-studied in recent years Jing et al. [2020], Ramakrishnan et al. [2018], Cadene et al. [2019a], Clark et al. [2019], Niu et al. [2021], Gat et al. [2020].

Spurious correlations sometimes shortcut an answer to an image, and other times question to an answer. CF-VQA Niu et al. [2021] was proposed to alleviate this problem by replacing natural indirect effect (NIE) with total indirect effect (TIE). Still, this method focuses only on language bias, ignores the visual information, and can also mislead the VQA model, resulting in CF-VQA sometimes giving its answer directly by uttering salient objects in the picture even if the answer obviously should be a number or "yes/no" according to the type of the question.

Recent studies suggest that memory and culture influence the perception of visual information in humans Lupyan et al. [2020], the problem that we illustrate in Fig. 1 with a famous example of Rubin’s vase Rubin [1915], where the same image can be perceived differently. The difference in preference and perception confounds VQA datasets, making them biased in data collection and annotation process Antol et al. [2015], Niu et al. [2021]. Therefore, VQA models fail to generalize as these confounders affect vision and language in datasets.

Contradicting those existing methods, we propose a new system called possible worlds VQA (PW-VQA) to address vision and language biases by removing the confounding effects of two modalities through a causal lens. After removing these effects captured through training, our model is less biased by either language or vision modality during test time. Furthermore, compared to other models, ours achieved significant performance improvement on the numerical questions, which used to be a struggling problem for previous methods.

Our contributions are as follows. 1) We propose a causal graph separating the problem into two sub-graphs of anticausal learning and an explain-away network. We simultaneously model the visual and linguistic biases through the explain-away network to distinguish between bad and good language and vision biases. We model the experience bias of the annotator as an unobserved confounder that influences the choice of question and answer pairs. 2) We propose a counterfactual approach to reduce these bad biases while keeping the good ones. To the best of our knowledge, our work is the first to propose a causal method to simultaneously alleviate language and vision biases. 3) We double the accuracy of the numerical questions, which has been an open question recently Niu et al. [2021].

2 Motivation and Background

Our method is motivated by Counterfactual VQA, CF-VQA Niu et al. [2021], which was motivated by Reducing Unimodal Biases for VQA, RUBi Cadene et al. [2019a]. We review these two methods and their evolution in 2.1 and 2.2 and then discuss their limitations in 2.3.

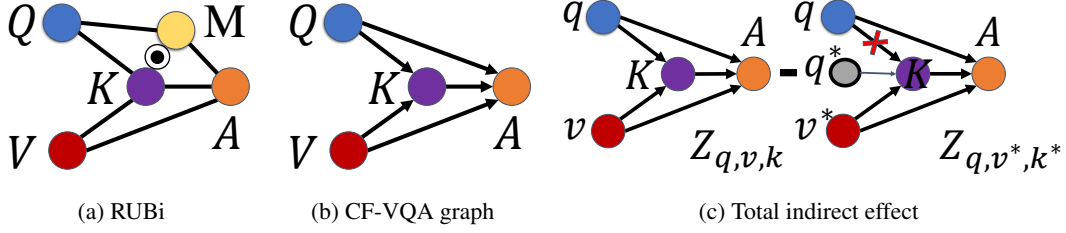


Figure 2: VQA graphs related to RUBi and CF-VQA are shown. a) In RUBi, question Q and image V are fused through multimodal knowledge K to obtain an answer A , while question-only mask M is applied on K ; b) causal graph of CF-VQA is shown, where $Q \rightarrow A$ and $V \rightarrow A$ are vision and language shortcuts, all V , Q , and K are factual; c) output of VQA with counterfactual question $Q = q^*$ and vision $V = v^*$ is subtracted from a regular VQA with factual $V = v$ and $Q = q$.

2.1 Reducing Unimodal Biases for VQA

The undirected graph of a RUBi is shown in Fig. 2a, with $\{V, Q, K, A, M\}$ as set of nodes, V : image, Q : question, K : multimodal knowledge, A : answer out of a set of answers $\mathcal{A} = \{a\}$, M : question mask. \mathcal{F}_Q is an encoder for questions, and \mathcal{F}_V is for images. Consequently, a multimodal function \mathcal{F}_{VQ} is used to obtain $k = \mathcal{F}_{VQ}(v, q)$. An auxiliary neural network nn_q is trained to classify answers based on only $\{q, a\}$ pairs. Then, the classification head is discarded at inference to obtain the masks $m = \sigma(nn_q(\mathcal{F}_Q(q)))$, where σ is the *sigmoid* function. The masks are then applied to the multimodal classification $k \odot m$ to reduce the language bias.

2.2 Counterfactual VQA (CF-VQA)

CF-VQA uses counterfactual thinking and causal inference to improve RUBi, by only adding one learnable parameter. The causal graph of CF-VQA is shown in Fig. 2b. The graph $\mathcal{G} = \{\mathcal{V}, \mathcal{E}\}$ is a Directed Acyclic Graph (DAG), where $\mathcal{V} = \{V, Q, K, A\}$ with a set of causal edges such that if $Q \rightarrow K$, then Q is a direct cause of K . Moreover, Q is an indirect cause of A through the *mediator* K , as $Q \rightarrow K \rightarrow A$. The causal edge assumption states that every parent is a direct cause of all its children. The answer a can be defined in a multi-class classifier using logits (score) Z . Therefore, for h as a fusion function, for question q , image v , and multimodal knowledge k , these scores for question-only, multimodal fused and vision-only are:

$$\begin{aligned} Z_q &= \mathcal{F}_Q(q), & Z_v &= \mathcal{F}_V(v), & Z_k &= \mathcal{F}_{VQ}(v, q), \\ Z_{q,v,k} &= h(Z_q, Z_v, Z_k), \end{aligned} \quad (1)$$

Denoting answer score $Z_{q,v,k}$ as:

$$Z_{q,v,k} = Z(Q = q, V = v, K = k), \quad (2)$$

the total effect (TE) of $V = v$ and $Q = q$ on $A = a$, according to Niu et al. [2021], is defined as:

$$TE = Z_{q,v,k} - Z_{q^*,v^*,k^*}, \quad (3)$$

where Z_{q^*,v^*,k^*} is answer logits Z for counterfactual question q^* , counterfactual image v^* , and counterfactual multimodal knowledge k^* . The total effect can be decomposed into natural direct effect (NDE) and total indirect effect

(TIE):

$$TE = TIE + NDE. \quad (4)$$

NDE for the question-only branch is $Q \rightarrow A$ by comparing Z_{q,v^*,k^*} and Z_{q^*,v^*,k^*} :

$$NDE = Z_{q,v^*,k^*} - Z_{q^*,v^*,k^*}. \quad (5)$$

Finally, using (3), (4), and (5), TIE will be:

$$TIE = Z_{q,v,k} - Z_{q,v^*,k^*}, \quad (6)$$

as shown in Fig. 2c. Consequently, the logits $Z_{q,v,k}$ is parametrized as $\mathcal{F}_Q: Q \rightarrow A$, and $\mathcal{F}_{VQ}: (V, Q) \rightarrow K \rightarrow A$. The question-only and vision-only logits Z_q and Z_v will be as:

$$Z_b = \begin{cases} z_b = \mathcal{F}_B(b) & \text{if } B = b \\ z_b^* = c & \text{if } b = \emptyset \end{cases}, \quad (7)$$

where $B \in \{Q, V\}$, and c as a constant, learnable feature, as described in Niu et al. [2021], and z_b^* is a counterfactual realization of Z_b . Furthermore, multimodal knowledge's logit Z_k is defined as:

$$Z_k = \begin{cases} z_k = \mathcal{F}_{VQ}(v, q) & \text{if } V = v \text{ and } Q = q \\ z_k^* = c & \text{if } V = \emptyset \text{ or } Q = \emptyset \end{cases}. \quad (8)$$

2.3 Limitations

Visual Bias in VQA: Visual bias is relatively recent, especially since the language has been known as the primary source of spurious question-answer correlations and has shadowed the research on vision bias Gat et al. [2020]. Some recent works have studied the VQA systems' shortcuts directly from the vision's contextual information to the answer Gupta et al. [2022]. This includes the learning biases of the colors and pixels or the context of the image and a lack of accurate attention to the important parts Gupta et al. [2022]. We propose a method that mitigates both the language and vision biases in a counterfactual explain-away network that enhances the multimodality of the VQA models.

Memory's Influence: Recent studies suggest that memory influences visual perception Lupyan et al. [2020], the problem that we illustrate with a famous example of Rubin's face Rubin [1915], as shown in Fig. 1, where the same image can be perceived differently. Rubin discussed this as memory bias Rubin [1915, 1921], which accumulates based on the experiences of individuals. The importance of visual perception may depend on the language Lupyan et al. [2020], location Zhang and Choi [2021], time Zhang and Choi [2021], and experiences of people Liu et al. [2021], which may lead to interpret an image in different ways. Although prior works on other datasets have tried to add concepts or new languages Liu et al. [2021], our work proposes a method to address the experience of the annotator as an unobserved confounder to reduce experience bias.

3 Possible Worlds VQA (PW-VQA)

In this section, we explain the proposed method in four subsections. First, we simultaneously model the language and vision bias using a causal view. Then we model experience bias as unobserved confounders of the VQA systems. Third, a counterfactual method is proposed in the subsequent subsection to solve these problems. Finally, we propose a novel strategy to fuse multimodal vision and language information in VQA systems.

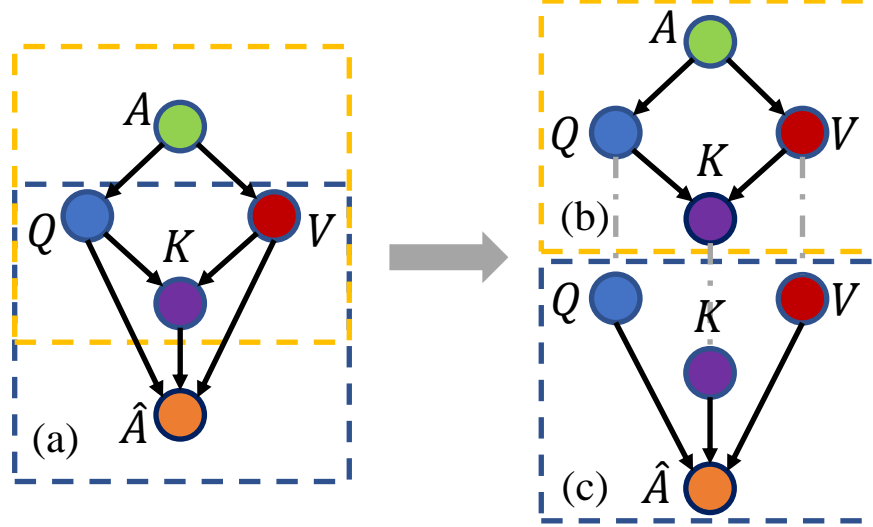


Figure 3: The proposed causal graph reformulates the VQA problem by stating that a) the answer A is a cause of the question Q , and vision V , and the final estimated answer \hat{A} is achieved by fusing V and Q information. b) The anticausal subgraph consists of the ground-truth answer A that is a cause of the V and Q , which leads to multimodal knowledge K . c) The collider $Q \rightarrow K \leftarrow V$ is an explain-away network that models the language-vision bias.

Assume that a multimodal knowledge K contains fused information of question Q and vision V used in a VQA system. We propose the causal graph $\mathcal{G} = \{\mathcal{V}, \mathcal{E}\}$ with the set of nodes $\mathcal{V} = \{Q, V, K, A, \hat{A}\}$, which is shown in Fig. 3a to model VQA systems.

Inspired by the anticausal learning Janzing et al. [2012], Arjovsky et al. [2019], we model the answer A as a cause of both the images V and question Q . Unlike previous works Niu et al. [2021], Cadene et al. [2019a], Niu and Zhang [2021], we distinguish between the ground-truth answer A for the training of the VQA model and the estimated answer \hat{A} when the model is used in practice (test). Therefore, as shown in Fig. 3b, Q and V have a causal effect on K and are also a child of the answer A .

Collider Confounder in Vision and Language: The relationship $Q \rightarrow A$ creates a spurious correlation between the question Q directly to the answer A . Therefore, the $V \rightarrow K \rightarrow A$ information is ignored. Contrarily the VQA models may shortcut visual information to answer $V \rightarrow K \rightarrow A$ rather than multimodal knowledge Gupta et al. [2022]. By looking at the subgraph shown in Fig. 3c, the explain-away network, or collider bias network simultaneously can model vision and language bias. The relationship $Q \rightarrow \hat{A} \leftarrow V$ is a collider, a primitive graph structure, *aka* explain-away network. Consequently, having a strong connection $Q \rightarrow \hat{A}$ removes the dependency of the \hat{A} on V . Noteworthy that there are useful information and harmful biases in both vision and language. Our explain-away method aims to remove biases but keep good information. Therefore we introduce the collider of $Q \rightarrow \hat{A} \leftarrow V$ as a source of vision-language

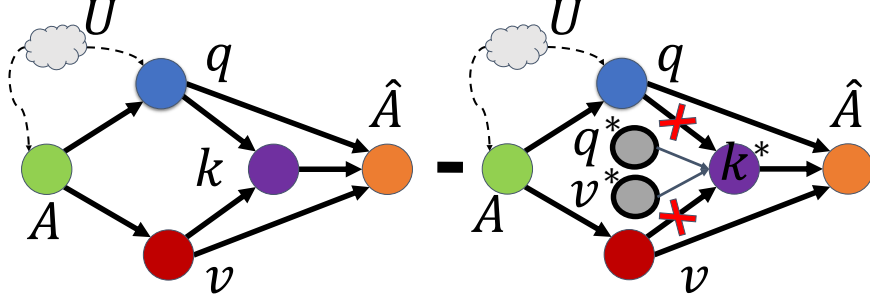


Figure 4: The multimodal knowledge $K = k^*$ is counterfactual, while Q and V are facts ($Q = q, V = v, K = k^*$), then, the natural indirect effect (NDE) is subtracted from the total effect (TE) to obtain total indirect effect (TIE). The values $V = v$ and $Q = q$ are fact, and $V = v^*$ and $Q = q^*$, which leads to $K = k^*$ are counterfactuals.

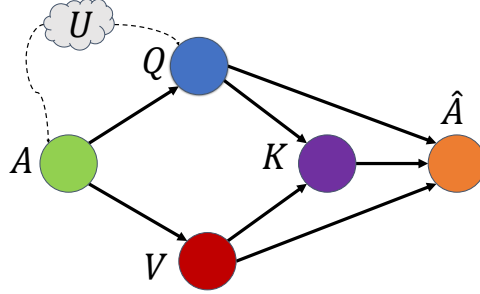


Figure 5: The causal graph of the VQA where the question Q and the answer A are influenced by unobserved confounder U .

bias in VQA models.

Experience as an Unobserved Confounder: Based on the proposed causal graph \mathcal{G} , a novel source of confounding is introduced related to the experience of the annotator that happens during the preparation of the datasets. As an example of experience bias, we have seen the visual illusion problem in Fig. 1. To be specific, selecting questions Q and answering A to the question based on an image V relies on the personal preferences of the annotator. Therefore, unobserved bias U depends on the personal preferences of the annotator. The proposed causal graph for the VQA models with unobserved confounder is shown in Fig. 5. Consequently, by looking into different paths that are parents or ancestors of \hat{A} , they can be listed as $U \rightarrow A \rightarrow Q \rightarrow K \rightarrow \hat{A}$, $U \rightarrow A \rightarrow Q \rightarrow K \rightarrow \hat{A}$, $U \rightarrow A \rightarrow V \rightarrow \hat{A}$, and $U \rightarrow A \rightarrow V \rightarrow K \rightarrow \hat{A}$. The same can be listed for $U \rightarrow Q$ paths; however, only $K \rightarrow \hat{A}$ is of interest for the VQA models.

Explain-Away Fusion Strategy (EA): We propose the following Explain-Away (EA) fusion function as follows. For parametrization, we use similar notations as Niu et al. [2021]. Therefore, the score $Z_{q,v,k}$ which is the feature space of the fusion K , is parametrized as $\mathcal{F}_Q: Q \rightarrow \hat{A}$, and $\mathcal{F}_{VQ}: (V, Q) \rightarrow K \rightarrow \hat{A}$.

Based on Z_q , Z_v , and Z_k , we define the fusion function as follows:

$$(EA) \quad h(Z_q, Z_v, Z_k) = \frac{1}{\alpha + 1} \log(Z_{EA}), \quad (9)$$

where Z_{EA} is defined as:

$$\begin{aligned} Z_{EA} = & \sigma(Z_q)^\alpha \sigma(Z_v)^{\alpha+1} \sigma(Z_k)^{\alpha+1} \\ & + \sigma(Z_q)^{\alpha+1} \sigma(Z_v)^\alpha \sigma(Z_k)^{\alpha+1} \\ & + \sigma(Z_q)^{\alpha+1} \sigma(Z_v)^{\alpha+1} \sigma(Z_k)^\alpha, \end{aligned} \quad (10)$$

and $\alpha \geq 0$ is a free parameter that can be defined based on empirical analysis.

Unobserved Confounding Bias Reduction: Since the model relies on the fused information K of V and Q , and as shown in Fig. 4, the confounding bias of vision-language can be removed by maximizing the total indirect effect (TIE) by subtracting natural direct effect (NDE) of this confounding influence from its total effect (TE) Pearl [2001]:

$$\begin{aligned} TIE &= TE - NDE \\ &= h(Z_q, Z_v, Z_k) - h(Z_q, Z_v, Z_{k^*}), \end{aligned} \quad (11)$$

where K^* is a counterfactual of K , as described in (8). As the influence of the unobserved confounding bias is subtracted in (11), it will block the influence of the explain-way of vision-language and experience biases altogether. By blocking the two paths $V \rightarrow K$ and $Q \rightarrow K$, all influences from unobserved confounding bias are blocked.

Training: For the training of the network, we use vision-only branch $\mathcal{L}_{VA}(v, a)$, question-only branch $\mathcal{L}_{QA}(q, a)$, and multimodal fusion branch $\mathcal{L}_{VQA}(v, q, a)$. As illustrated in Fig. 5, given a triplet (v, q, a) where a is the ground-truth answer of image-question pair (v, q) , the branches are optimized by minimizing the cross-entropy losses over the scores $Z_{q,v,k}$, Z_q and Z_v : Niu et al. [2021]:

$$\mathcal{L}_{cls} = \mathcal{L}_{VQA}(v, q, a) + \mathcal{L}_{QA}(q, a) + \mathcal{L}_{VA}(v, a), \quad (12)$$

where \mathcal{L}_{VQA} , \mathcal{L}_{QA} and \mathcal{L}_{VA} are over $Z_{q,v,k}$, Z_q and Z_v . A learnable parameter c in Eq. (7)-(8), which controls the sharpness of the distribution of Z_{q,v^*,k^*} is also included, as the sharpness of NDE should be similar to that of TE Hinton et al. [2015], Niu et al. [2021]. An improper c would lead to the domination of TIE in Eq. (11) by either TE or NDE. Thus, we use KL-divergence to estimate c :

$$\mathcal{L}_{kl} = \frac{1}{|\mathcal{A}|} \sum_{a \in \mathcal{A}} -p(a|q, v, k) \log p(a|q, v^*, k^*), \quad (13)$$

where $p(a|q, v, k) = \text{softmax}(Z_{q,v,k})$ and $p(a|q, v^*, k^*) = \text{softmax}(Z_{q,v^*,k^*})$. Only c is updated when minimizing \mathcal{L}_{kl} . The final loss is the combination of \mathcal{L}_{cls} and \mathcal{L}_{kl} :

$$\mathcal{L}_{final} = \sum_{(v,q,a) \in \mathcal{D}} \mathcal{L}_{cls} + \mathcal{L}_{kl} \quad (14)$$

Inference. For the inference, we use the debiased causal effect for inference, which is implemented as:

$$\begin{aligned} TIE &= TE - NDE = Z_{q,v,k} - Z_{q,v^*,k^*} \\ &= h(z_q, z_v, z_k) - h(z_q, z_v^*, z_k^*). \end{aligned} \quad (15)$$

Table 1: The table lists the accuracy values for the most recent studies, especially on both VQA-CP v2 and VQA v2 datasets. We show the best-performing method with bold and the second-best-performing method with an underline. We use a dash for the papers that miss reporting performance values on datasets.

Test set Methods	Base	VQA-CP v2 test				VQA v2 test			
		All	Y/N	Num.	Other	All	Y/N	Num.	Other
GVQA [Agrawal et al., 2018]	-	31.30	57.99	13.68	22.14	42.24	72.03	31.17	34.65
SAN [Yang et al., 2016]	-	24.96	38.35	11.14	21.74	52.41	70.06	39.28	47.84
UpDn [Anderson et al., 2018]	-	39.74	42.27	11.93	46.05	63.48	81.18	42.14	55.66
S-MRL [Cadene et al., 2019a]	-	38.46	42.85	12.81	43.20	63.10	-	-	-
<i>Methods based on modifying language module or using language prior:</i>									
DLR [Jing et al., 2020]	UpDn	48.87	70.99	18.72	45.57	57.96	76.82	39.33	48.54
VGQE [Kv and Mittal, 2020]	UpDn	48.75	-	-	-	64.04	-	-	-
VGQE [Kv and Mittal, 2020]	S-MRL	50.11	66.35	27.08	46.77	63.18	-	-	-
AdvReg. [Ramakrishnan et al., 2018]	UpDn	41.17	65.49	15.48	35.48	62.75	79.84	42.35	55.16
RUBi [Cadene et al., 2019a]	UpDn	44.23	67.05	17.48	39.61	-	-	-	-
RUBi [Cadene et al., 2019a]	S-MRL	47.11	68.65	20.28	43.18	61.16	-	-	-
LM [Clark et al., 2019]	UpDn	48.78	72.78	14.61	45.58	63.26	81.16	42.22	55.22
LM+H [Clark et al., 2019]	UpDn	52.01	72.58	31.12	46.97	56.35	65.06	37.63	54.69
CF-VQA (SUM) [Niu et al., 2021]	UpDn	53.55	91.15	13.03	44.97	<u>63.54</u>	82.51	43.96	54.30
CF-VQA (SUM) [Niu et al., 2021]	S-MRL	55.05	<u>90.61</u>	21.50	45.61	<u>60.94</u>	81.13	43.86	50.11
GGE-DQ-tog [Han et al., 2021]	UpDn	57.32	87.04	27.75	49.59	59.11	73.27	39.99	54.39
<i>Methods based on reducing visual bias or enhancing visual attention/grounding:</i>									
AttAlign [Selvaraju et al., 2019]	UpDn	39.37	43.02	11.89	45.00	63.24	80.99	42.55	55.22
HINT [Selvaraju et al., 2019]	UpDn	46.73	67.27	10.61	45.88	63.38	81.18	42.99	<u>55.56</u>
SCR [Wu and Mooney, 2019]	UpDn	49.45	72.36	10.93	<u>48.02</u>	62.20	78.80	41.60	54.50
<i>Methods mitigating both language and vision:</i>									
LMH+Fisher [Gat et al., 2020]	UpDn	54.55	74.03	49.16	45.82	-	-	-	-
PW-VQA (ours)	UpDn	<u>59.06</u>	88.26	<u>52.89</u>	45.45	62.63	<u>81.80</u>	<u>43.90</u>	53.01
PW-VQA (ours)	S-MRL	60.26	88.09	59.13	45.99	61.25	80.32	43.17	51.53
<i>Methods that synthesize data to augment and balance training splits:</i>									
CVL [Abbasnejad et al., 2020]	UpDn	42.12	45.72	12.45	48.34	-	-	-	-
Unshuffling [Teney et al., 2020a]	UpDn	42.39	47.72	14.43	47.24	68.08	78.32	42.16	52.81
RandImg [Teney et al., 2020b]	UpDn	55.37	83.89	41.60	44.20	57.24	76.53	33.87	48.57
SSL [Zhu et al., 2021]	UpDn	57.59	86.53	29.87	50.03	63.73	-	-	-
CSS [Chen et al., 2020]	UpDn	58.95	84.37	49.42	48.21	59.91	73.25	39.77	55.11
CSS+CL [Liang et al., 2020]	UpDn	59.18	86.99	49.89	47.16	57.29	67.27	38.40	54.71
Mutant [Gokhale et al., 2020]	UpDn	61.72	88.90	49.68	50.78	62.56	82.07	42.52	53.28
LMH+ECD [Kolling et al., 2022]	UpDn	59.92	83.23	52.59	49.71	57.38	69.06	35.74	54.25

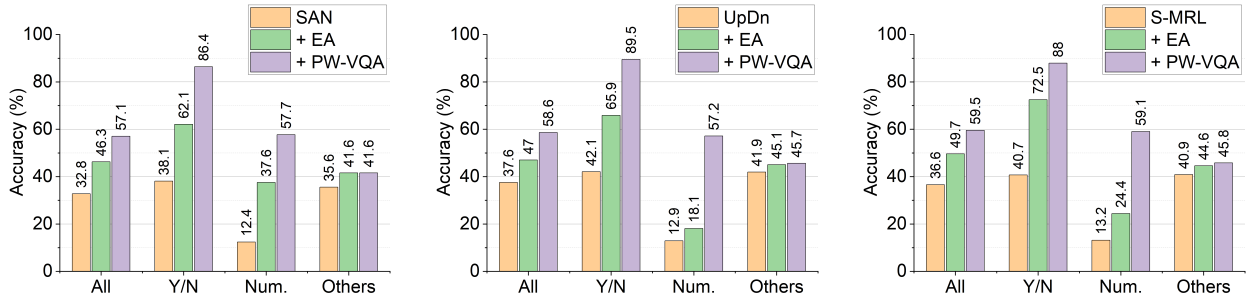


Figure 6: The plots show the backbones using our proposed causal framework (PW-VQA) and fusion strategy (EA). The results are consistently improving for all three different backbones, namely, SAN Yang et al. [2016], S-MRL Cadene et al. [2019a], and UpDn Anderson et al. [2018].

4 Experiments

The model can be trained on a computer with a single GeForce GTX 1080 GPU. We used GTX 1080 Ti and RTX A6000 GPUs in our simulations. We used the VQA-CP v2 dataset, which has about 438K questions on the train set and 220K questions on the test set, with corresponding question-answer pairs in the English language Agrawal et al. [2018]. We applied our VQA model on three backbones, namely Stacked Attention Network (SAN) Yang et al. [2016], Bottom-up and Top-down Attention (UpDn) Anderson et al. [2018], and a simplified MUREL Cadene et al. [2019b]

(S-MRL) Cadene et al. [2019a]. Training of our model on VQA-CP v2 dataset Agrawal et al. [2018] with SAN Yang et al. [2016] takes about 8 hours, and with S-MRL Cadene et al. [2019a] and UpDn Anderson et al. [2018] on average takes about 3 hours. The validation on the test split of the VQA-CP v2 dataset takes about 10 minutes. We used accuracy as the evaluation metric. We manually searched the hyperparameter, and we reported those which have the best results in the ablation study. We used a batch size of 256 and 22 epochs for all runs. Increasing the number of epochs does not improve the results since the model converges to a stable result within 22 epochs. We observed that the model does not converge with $\alpha < 1$ values, and therefore we bound $\alpha \geq 1$. We tried α values between 1 to 2 for 11 times and based on empirical study, $\alpha = 1.5$ achieves the best-performing result.

Quantitative results: To compare our method with the available literature on the benchmark datasets, we list the performance values in Table 1. Then, to compare reasonably with the existing methods, we divide them into four categories: 1) Methods like DLR Jing et al. [2020], VGQE Kv and Mittal [2020]), AdvReg Ramakrishnan et al. [2018], RUBi Cadene et al. [2019a], LM Clark et al. [2019], LM+H Clark et al. [2019], CF-VQANiu et al. [2021], GGE-DQ-tog Han et al. [2021] modify language modules or use language before suppress, control, or mask language shortcuts. However, these methods only consider spurious language correlations and neglect vision in their schema. 2) Some approaches, such as AttAlign Selvaraju et al. [2019], HINT Selvaraju et al. [2019], SCR Wu and Mooney [2019] mitigate visual biases by loosening contextual ties to the answer or improving visual grounding and attention via human feedback, de-coupling shortcuts that couple vision to answer. 3) Other approaches like LMH+Fisher Gat et al. [2020] mitigate both language and vision bias together, attempting to balance two modalities of vision and language for robust multimodal inference. Our proposed method here is in this class. 4) Methods such as CVL Abbasnejad et al. [2020], Unshuffling Teney et al. [2020a], RandImg Teney et al. [2020b], SSL Zhu et al. [2021], Mutant Gokhale et al. [2020], CSS Chen et al. [2020], CSS+CL Liang et al. [2020], LMH+ECD Kolling et al. [2022] synthesize samples and augment data to balance training and test sets; however, it violates the main idea of the VQA-CP v2 dataset. Therefore, it is not fair to compare them with our method; however, we include them in our results for inclusiveness.

As listed in Table 1, our method outperforms most of the competing methods on the benchmark datasets, especially in numerical questions, which was introduced as an open problem recently Niu et al. [2021]. Moreover, the results indicate that our method improves the accuracy of both the S-MRL and UpDn backbones, demonstrating that they are generalizable to both architectures. Noteworthy to mention that there are higher accuracy values for methods that augment data. In contrast, these methods are not comparable to ours as they do not obey the main idea of the VQA-CP v2 dataset, conducting unbiased inference under biased training. Simulation results of our proposed EA fusion strategy and the PW-VQA are shown in Fig. 6. Both the EA fusion strategy and PW-VQA framework increase the accuracy of all question types. Particularly, the accuracy of numerical results with SAN as backbone increases from 12.4 to 37.6 by adding EA fusion and further increases to 57.7 by adding the PW-VQA framework. Furthermore, the improvements are consistent for all backbones, including SAN, S-MRL, and UpDn. More improvements can be achieved using large pretrained language-vision models. We used generative BLIP decoder Li et al. [2022] and CLIP encoders Radford et al. [2021] to achieve more improvements.²

Qualitative results To qualitatively show the results of our method vs CF-VQA and regular VQA, we did simulations

²For more explanations see the appendix.

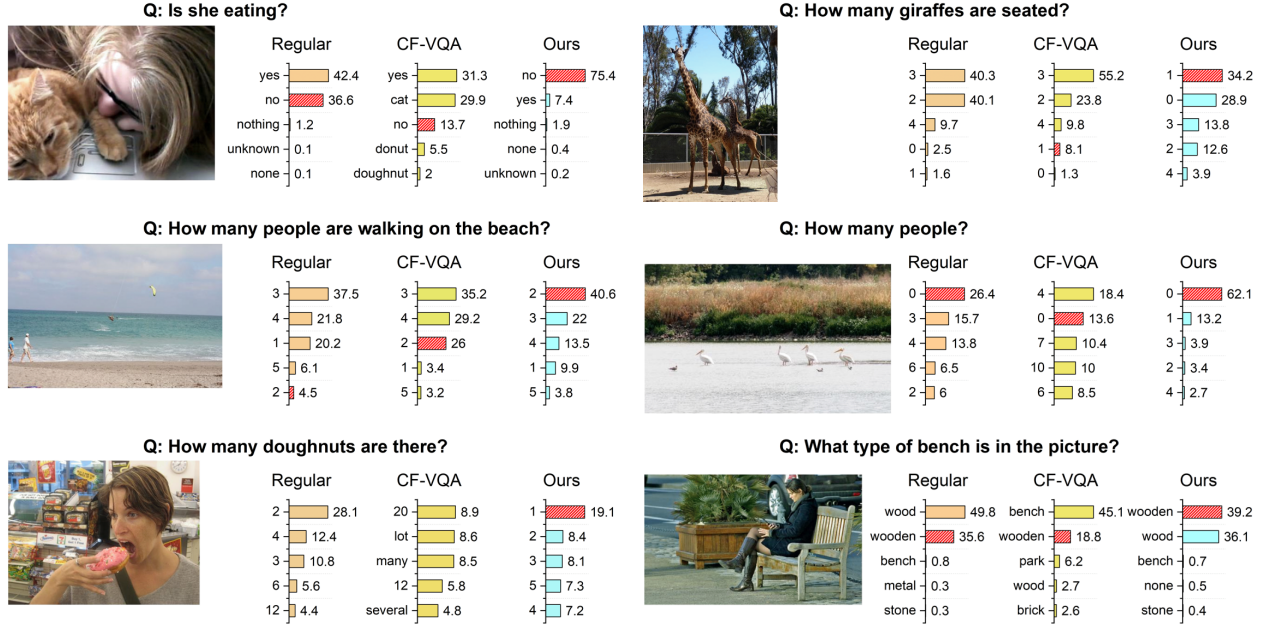


Figure 7: Qualitative comparison on VQA-CP v2 test split on regular VQA, CF-VQA Niu et al. [2021] and our method are shown as bar plots, where the red bars with a sparse pattern are ground-truth. Values on the bars are probabilities out of 100% to have an answer as correct.

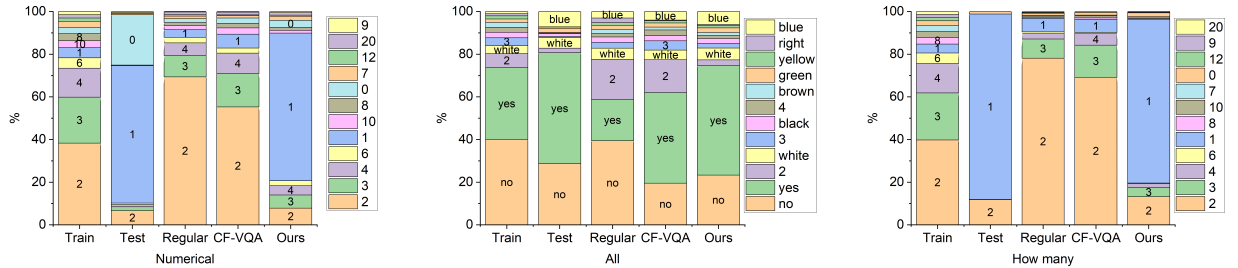


Figure 8: The distributions of the train, test sets, the previous methods, namely regular VQA, CF-VQA Niu et al. [2021], and our proposed method are shown. Note that there is a subtle difference between "how many" questions versus questions with "numerical" answers, which is related to the difference between recognizing "numerical" rather than counting "how many".

on the VQA-CP v2 dataset which, some examples have been shown in Fig. 7. As seen in the pictures of Fig. 7, our method is less biased by either language or vision bias. For example, When asked, "Is she eating?" for a picture showing a cat and a woman, our method can correctly answer "No" while the regular VQA cannot. Interestingly, the CF-VQA is clearly biased by the salient object in the picture and has extremely high confidence in answering this question with "cat" which is obviously ridiculous. Another example is both regular VQA and CF-VQA cannot use the key information from the question, which results in answering the question with biased inference due to the foreground animals in the picture. More examples are in the appendix.

Five distributions of numerical answers for train, test, regular VQA, CF-VQA, and our model are shown in Fig. 8. We can clearly see in Fig. 8 that CF-VQA captured many biases in question with "numerical" answers from the training

dataset. At the same time, our model reduces those biases and obtains answer distribution benefits from removing language and vision biases simultaneously during de-confounding causal inference and closer to the test dataset.

5 Related Work

VQA-CP dataset has been proposed to benchmark the generalizability of VQA models under changing prior conditions Agrawal et al. [2018]. Various methods Niu et al. [2021], Han et al. [2021], Gat et al. [2020], Kv and Mittal [2020], Abbasnejad et al. [2020], Kolling et al. [2022], Gupta et al. [2022], Shrestha et al. [2022] have been proposed to solve VQA-CP, which can be divided into four main categories. 1) Methods that modify language module or use language prior to suppressing or controlling language shortcuts by separating question-only branches or capturing language prior to subtracting or masking in the model Ramakrishnan et al. [2018], Cadene et al. [2019a], Clark et al. [2019]. 2) Methods that mitigate bias through reducing visual bias or enhancing visual attention/grounding use human input to increase the attention to visual information or reduce contextual biases that shortcut vision to answer Selvaraju et al. [2019], Wu and Mooney [2019], Das et al. [2017]. 3) Mitigation of both language and vision bias together that tries to balance two modalities of vision and language for robust multimodal inference. And 4) Methods that synthesize data to augment and balance training splits, that use generative models to synthesize and augment visual and linguistic data to balance the distribution of training splits Chen et al. [2020], Abbasnejad et al. [2020], Teney et al. [2020a], Zhu et al. [2021], Kolling et al. [2022].

The causal inference has inspired several studies in computer vision, including visual explanations Goyal et al. [2019], Wang and Vasconcelos [2020], Yi et al. [2019], scene graph generation Tang et al. [2020], image recognition Tang et al. [2020], zero-shot and few-shot learning Yue et al. [2020, 2021] incremental learning Hu et al. [2021], representation learning Wang et al. [2020], Zhang et al. [2020a], semantic segmentation Zhang et al. [2020b], and vision-language tasks Chen et al. [2020], Teney et al. [2020c], Yang et al. [2021a], Fu et al. [2020], Yang et al. [2021b]. Especially, counterfactual learning has been exploited in recent VQA studies Chen et al. [2020], Teney et al. [2020c], Abbasnejad et al. [2020].

6 Conclusion

VQA systems suffer from leveraging information only from one modality, especially the language modality from the given question. Many methods have been proposed to address this kind of problem. However, the previous method didn't consider that biases that come from each modality are highly confounded through the annotation process. VQA systems that ignore this effect cannot avoid increasing the bias learned from one modality while trying to reduce bias from another modality. We formulate the Explain-Away effect that causes the bias of both vision and language modalities with a novel causal framework for VQA systems. This framework can be implemented on the different VQA backbones and improve their generalizability significantly. The proposed framework successfully helps VQA systems reduce language bias without increasing vision bias. Experiment results show that our proposed method

achieved state-of-the-art performance on de-bias oriented dataset VQA-CP especially doubled the accuracy on numerical questions from the previous best model.

Acknowledgments

This work has been partially supported by the National Science Foundation (NSF) under Grant 1909912 and the Defense Advance Research Projects Agency (DARPA) under Contract HR00112220003. The content of the information does not necessarily reflect the position of the Government, and no official endorsement should be inferred.

References

- Gary Lupyan, Rasha Abdel Rahman, Lera Boroditsky, and Andy Clark. Effects of language on visual perception. *Trends in cognitive sciences*, 24(11):930–944, 2020.
- Edgar Rubin. Synsoplevede figurer. 1915.
- Rowan Zellers, Yonatan Bisk, Ali Farhadi, and Yejin Choi. From recognition to cognition: Visual commonsense reasoning. In *Proceedings of the IEEE Conference on Computer Vision and Pattern Recognition*, pages 6720–6731, 2019.
- Yulei Niu, Kaihua Tang, Hanwang Zhang, Zhiwu Lu, Xian-Sheng Hua, and Ji-Rong Wen. Counterfactual vqa: A cause-effect look at language bias. In *CVPR*, pages 12700–12710, 2021.
- Camila Kolling, Martin More, Nathan Gavenski, Eduardo Pooch, Otávio Parraga, and Rodrigo C Barros. Efficient counterfactual debiasing for visual question answering. In *Proceedings of the IEEE/CVF Winter Conference on Applications of Computer Vision*, pages 3001–3010, 2022.
- Yulei Niu and Hanwang Zhang. Introspective distillation for robust question answering. *Advances in Neural Information Processing Systems*, 34:16292–16304, 2021.
- Remi Cadene, Corentin Dancette, Matthieu Cord, Devi Parikh, et al. Rubi: Reducing unimodal biases for visual question answering. *Advances in Neural Information Processing Systems*, 32:841–852, 2019a.
- Remi Cadene, Hedi Ben-Younes, Matthieu Cord, and Nicolas Thome. Murel: Multimodal relational reasoning for visual question answering. In *Proceedings of the IEEE Conference on Computer Vision and Pattern Recognition*, pages 1989–1998, 2019b.
- Chenchen Jing, Yuwei Wu, Xiaoxun Zhang, Yunde Jia, and Qi Wu. Overcoming language priors in vqa via decomposed linguistic representations. In *AAAI*, pages 11181–11188, 2020.
- Sainandan Ramakrishnan, Aishwarya Agrawal, and Stefan Lee. Overcoming language priors in visual question answering with adversarial regularization. In *Advances in Neural Information Processing Systems*, pages 1541–1551, 2018.
- Christopher Clark, Mark Yatskar, and Luke Zettlemoyer. Don’t take the easy way out: Ensemble based methods for avoiding known dataset biases. In *Proceedings of the 2019 Conference on Empirical Methods in Natural Language*

- Processing and the 9th International Joint Conference on Natural Language Processing (EMNLP-IJCNLP)*, pages 4060–4073, 2019.
- Itai Gat, Idan Schwartz, Alexander Schwing, and Tamir Hazan. Removing bias in multi-modal classifiers: Regularization by maximizing functional entropies. *Advances in Neural Information Processing Systems*, 33:3197–3208, 2020.
- Stanislaw Antol, Aishwarya Agrawal, Jiasen Lu, Margaret Mitchell, Dhruv Batra, C. Lawrence Zitnick, and Devi Parikh. VQA: Visual Question Answering. In *International Conference on Computer Vision (ICCV)*, 2015.
- Vipul Gupta, Zhuowan Li, Adam Kortylewski, Chenyu Zhang, Yingwei Li, and Alan Yuille. Swapmix: Diagnosing and regularizing the over-reliance on visual context in visual question answering. In *Proceedings of the IEEE/CVF Conference on Computer Vision and Pattern Recognition*, pages 5078–5088, 2022.
- Edgar Rubin. *Visuell wahrgenommene figuren: Studien in psychologischer analyse*, volume 1. Gyldendalske boghandel, 1921.
- Michael Zhang and Eunsol Choi. Situatedqa: Incorporating extra-linguistic contexts into qa. In *Proceedings of the 2021 Conference on Empirical Methods in Natural Language Processing*, pages 7371–7387, 2021.
- Fangyu Liu, Emanuele Bugliarello, Edoardo Maria Ponti, Siva Reddy, Nigel Collier, and Desmond Elliott. Visually grounded reasoning across languages and cultures. In *Proceedings of the 2021 Conference on Empirical Methods in Natural Language Processing*, pages 10467–10485, 2021.
- Dominik Janzing, Jonas Peters, Eleni Sgouritsa, Kun Zhang, Joris M Mooij, and Bernhard Schölkopf. On causal and anticausal learning. In *Proceedings of the 29th International Conference on Machine Learning (ICML-12)*, pages 1255–1262, 2012.
- Martin Arjovsky, Léon Bottou, Ishaan Gulrajani, and David Lopez-Paz. Invariant risk minimization. *arXiv preprint arXiv:1907.02893*, 2019.
- Judea Pearl. Direct and indirect effects. *Probabilistic and Causal Inference*, 2001.
- Geoffrey Hinton, Oriol Vinyals, and Jeff Dean. Distilling the knowledge in a neural network. *arXiv preprint arXiv:1503.02531*, 2015.
- Aishwarya Agrawal, Dhruv Batra, Devi Parikh, and Aniruddha Kembhavi. Don’t just assume; look and answer: Overcoming priors for visual question answering. In *Proceedings of the IEEE Conference on Computer Vision and Pattern Recognition*, pages 4971–4980, 2018.
- Zichao Yang, Xiaodong He, Jianfeng Gao, Li Deng, and Alex Smola. Stacked attention networks for image question answering. In *Proceedings of the IEEE conference on computer vision and pattern recognition*, pages 21–29, 2016.
- Peter Anderson, Xiaodong He, Chris Buehler, Damien Teney, Mark Johnson, Stephen Gould, and Lei Zhang. Bottom-up and top-down attention for image captioning and visual question answering. In *Proceedings of the IEEE Conference on Computer Vision and Pattern Recognition*, pages 6077–6086, 2018.
- Gouthaman Kv and Anurag Mittal. Reducing language biases in visual question answering with visually-grounded question encoder. In *European Conference on Computer Vision*, pages 18–34. Springer, 2020.

- Xinzhe Han, Shuhui Wang, Chi Su, Qingming Huang, and Qi Tian. Greedy gradient ensemble for robust visual question answering. In *Proceedings of the IEEE/CVF International Conference on Computer Vision*, pages 1584–1593, 2021.
- Ramprasaath R Selvaraju, Stefan Lee, Yilin Shen, Hongxia Jin, Shalini Ghosh, Larry Heck, Dhruv Batra, and Devi Parikh. Taking a hint: Leveraging explanations to make vision and language models more grounded. In *Proceedings of the IEEE/CVF International Conference on Computer Vision*, pages 2591–2600, 2019.
- Jialin Wu and Raymond Mooney. Self-critical reasoning for robust visual question answering. *Advances in Neural Information Processing Systems*, 32, 2019.
- Ehsan Abbasnejad, Damien Teney, Amin Parvaneh, Javen Shi, and Anton van den Hengel. Counterfactual vision and language learning. In *Proceedings of the IEEE/CVF Conference on Computer Vision and Pattern Recognition*, pages 10044–10054, 2020.
- Damien Teney, Ehsan Abbasnejad, and Anton van den Hengel. Unshuffling data for improved generalization. *arXiv preprint arXiv:2002.11894*, 2020a.
- Damien Teney, Ehsan Abbasnejad, Kushal Kafle, Robik Shrestha, Christopher Kanan, and Anton Van Den Hengel. On the value of out-of-distribution testing: An example of goodhart’s law. *Advances in Neural Information Processing Systems*, 33:407–417, 2020b.
- Xi Zhu, Zhendong Mao, Chunxiao Liu, Peng Zhang, Bin Wang, and Yongdong Zhang. Overcoming language priors with self-supervised learning for visual question answering. pages 1083–1089, 2021.
- Long Chen, Xin Yan, Jun Xiao, Hanwang Zhang, Shiliang Pu, and Yueting Zhuang. Counterfactual samples synthesizing for robust visual question answering. In *Proceedings of the IEEE/CVF Conference on Computer Vision and Pattern Recognition*, pages 10800–10809, 2020.
- Zujie Liang, Weitao Jiang, Haifeng Hu, and Jiaying Zhu. Learning to contrast the counterfactual samples for robust visual question answering. In *Proceedings of the 2020 Conference on Empirical Methods in Natural Language Processing (EMNLP)*, pages 3285–3292, 2020.
- Tejas Gokhale, Pratyay Banerjee, Chitta Baral, and Yezhou Yang. Mutant: A training paradigm for out-of-distribution generalization in visual question answering. In *Proceedings of the 2020 Conference on Empirical Methods in Natural Language Processing (EMNLP)*, pages 878–892, 2020.
- Junnan Li, Dongxu Li, Caiming Xiong, and Steven Hoi. Blip: Bootstrapping language-image pre-training for unified vision-language understanding and generation. In *ICML*, 2022.
- Alec Radford, Jong Wook Kim, Chris Hallacy, Aditya Ramesh, Gabriel Goh, Sandhini Agarwal, Girish Sastry, Amanda Askell, Pamela Mishkin, Jack Clark, et al. Learning transferable visual models from natural language supervision. In *International Conference on Machine Learning*, pages 8748–8763. PMLR, 2021.
- Robik Shrestha, Kushal Kafle, and Christopher Kanan. An investigation of critical issues in bias mitigation techniques. In *Proceedings of the IEEE/CVF Winter Conference on Applications of Computer Vision*, pages 1943–1954, 2022.

- Abhishek Das, Harsh Agrawal, Larry Zitnick, Devi Parikh, and Dhruv Batra. Human attention in visual question answering: Do humans and deep networks look at the same regions? *Computer Vision and Image Understanding*, 163:90–100, 2017.
- Yash Goyal, Ziyang Wu, Jan Ernst, Dhruv Batra, Devi Parikh, and Stefan Lee. Counterfactual visual explanations. In *International Conference on Machine Learning*, pages 2376–2384. PMLR, 2019.
- Pei Wang and Nuno Vasconcelos. Scout: Self-aware discriminant counterfactual explanations. In *Proceedings of the IEEE/CVF Conference on Computer Vision and Pattern Recognition*, pages 8981–8990, 2020.
- Kexin Yi, Chuhan Gan, Yunzhu Li, Pushmeet Kohli, Jiajun Wu, Antonio Torralba, and Joshua B Tenenbaum. Clevrer: Collision events for video representation and reasoning. *arXiv preprint arXiv:1910.01442*, 2019.
- Kaihua Tang, Yulei Niu, Jianqiang Huang, Jiaxin Shi, and Hanwang Zhang. Unbiased scene graph generation from biased training. In *Proceedings of the IEEE/CVF Conference on Computer Vision and Pattern Recognition*, pages 3716–3725, 2020.
- Zhongqi Yue, Hanwang Zhang, Qianru Sun, and Xian-Sheng Hua. Interventional few-shot learning. *Advances in neural information processing systems*, 33:2734–2746, 2020.
- Zhongqi Yue, Tan Wang, Qianru Sun, Xian-Sheng Hua, and Hanwang Zhang. Counterfactual zero-shot and open-set visual recognition. In *Proceedings of the IEEE/CVF Conference on Computer Vision and Pattern Recognition*, pages 15404–15414, 2021.
- Xinting Hu, Kaihua Tang, Chunyan Miao, Xian-Sheng Hua, and Hanwang Zhang. Distilling causal effect of data in class-incremental learning. In *Proceedings of the IEEE/CVF Conference on Computer Vision and Pattern Recognition*, pages 3957–3966, 2021.
- Tan Wang, Jianqiang Huang, Hanwang Zhang, and Qianru Sun. Visual commonsense r-cnn. In *Proceedings of the IEEE/CVF Conference on Computer Vision and Pattern Recognition*, pages 10760–10770, 2020.
- Shengyu Zhang, Tan Jiang, Tan Wang, Kun Kuang, Zhou Zhao, Jianke Zhu, Jin Yu, Hongxia Yang, and Fei Wu. Devlbart: Learning deconfounded visio-linguistic representations. In *Proceedings of the 28th ACM International Conference on Multimedia*, pages 4373–4382, 2020a.
- Dong Zhang, Hanwang Zhang, Jinhui Tang, Xian-Sheng Hua, and Qianru Sun. Causal intervention for weakly-supervised semantic segmentation. *Advances in Neural Information Processing Systems*, 33:655–666, 2020b.
- Damien Teney, Ehsan Abbasnejad, and Anton van den Hengel. Learning what makes a difference from counterfactual examples and gradient supervision. In *European Conference on Computer Vision*, pages 580–599. Springer, 2020c.
- Xu Yang, Hanwang Zhang, and Jianfei Cai. Deconfounded image captioning: A causal retrospect. *IEEE Transactions on Pattern Analysis and Machine Intelligence*, 2021a.
- Tsu-Jui Fu, Xin Wang, Scott Grafton, Miguel Eckstein, and William Yang Wang. Iterative language-based image editing via self-supervised counterfactual reasoning. In *Proceedings of the 2020 Conference on Empirical Methods in Natural Language Processing (EMNLP)*, pages 4413–4422, 2020.

Xu Yang, Hanwang Zhang, Guojun Qi, and Jianfei Cai. Causal attention for vision-language tasks. pages 9847–9857, 2021b.

Limitations

For questions and images that require background knowledge, PW-VQA fails to answer correctly. Indeed, CF-VQA and regular VQA also fail, as shown in Fig. 9. For instance, the answer to the question "What year was this picture taken?" requires background knowledge of details such as the years that those sneakers and bicycles were used. Given this knowledge, the answer may be accurate within a range, for instance, 1960-1980, which requires open-ended answers with visual reasoning of small and large details in both image and language. Likewise, the "what bridge is this?" answer requires background knowledge. Overall, our method and all other VQA systems require background knowledge to answer some questions.

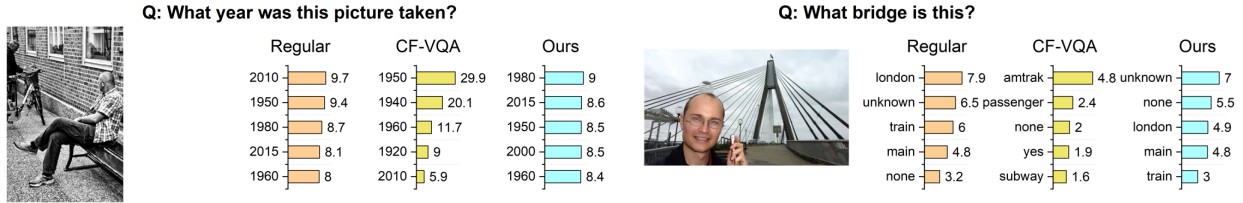


Figure 9: A limitation of VQA models is shown with two examples where PW-VQA fails to answer correctly; however, CF-VQA and regular VQA also fail.

Ethics Statement

VQA systems are fundamental building blocks in many AI systems, including visual dialog and question-answering systems. Therefore, any unethical information from the system, such as racial or gender-related problems, may have adverse social impacts if used at scale. Overall, VQA systems are helpful as AI assistants can aid people with disability or visual impairments or be used for visual queries with natural language interfaces.

A Appendix

A.1 Architecture of the PW-VQA

For the page limit considerations, we moved the PW-VQA framework’s architecture to here, shown in Fig. 10. The framework consists of two branches: regular VQA, which can be of any baseline method, and the counterfactual version of the same network and parameters, shown as a biased branch in the figure. Four different losses are simultaneously used during training to formulate the causal relationship between each modality. In addition, a constant c is jointly trained here to capture the natural indirect effect of vision-language confounding biased injected during the annotation

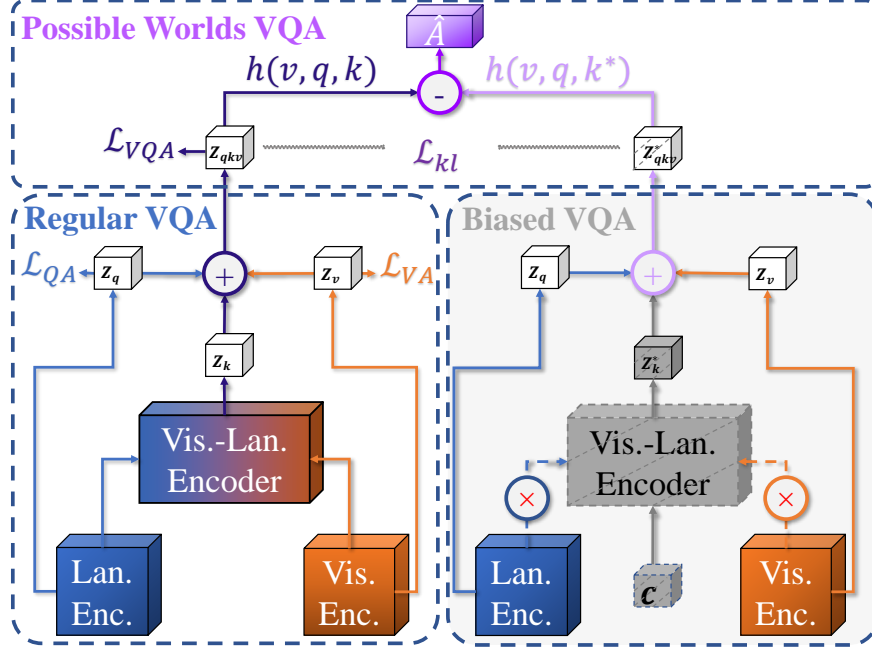


Figure 10: The image demonstrates our proposed PW-VQA framework.

process. Finally, in the inference stage, PW-VQA uses the logits of regular VQA subtracted by the biased VQA and gets a debiased answer. The letters a in this figure denote the answer.

A.2 Details on CLIP-BLIP model as baseline and results

Contrastive Language-Image Pretraining (CLIP) is a model trained on large image-text pairs with a contrasting loss Radford et al. [2021]. We use CLIP as the baseline for implementation as an ablation study on large pretrained vision-language models. Our implementation uses CLIP as a text and image encoder without fine-tuning. During the training, we use (v, q, a) ground-truth tuples and tokenize both question and answer. Then use CLIP to encode text and question tokens and normalize their sum. Then we use the CLIP image encoder and normalize features to embed images for the classification. We also use MLP layers to obtain logits of vision-only and language-only branches to later use in PW-VQA. The fusion of image and language is based on concatenation, and an MLP is used to obtain output vision-language logits. During inference, we use Bootstrapping Language-Image Pre-training for Unified Vision-Language Understanding and Generation (BLIP) Li et al. [2022], a generative pretrained model for open-ended visual question answering, and then use CLIP tokenizer and encoder to obtain language-only and vision-only and language-vision logits to be used in PW-VQA. As BLIP uses questions and images to generate open-ended answers, we use zero tensors as image inputs to the BLIP model to avoid spilling image features to question-only logits. Finally, CLIP features are normalized and used in the framework. Results for the BLIP-CLIP model as the baseline and other models are listed in Tab. 2. Although the accuracy of the BLIP-CLIP is significantly higher when used as a baseline, it cannot be compared with the other baselines, as BLIP is pretrained on more than 400 million image-text pairs, some of which are high-quality data. Similarly, CLIP is pretrained on large datasets of image-text pairs that have high-quality image-text pairs. Figure 11 shows the architecture of the implemented CLIP-BLIP model.

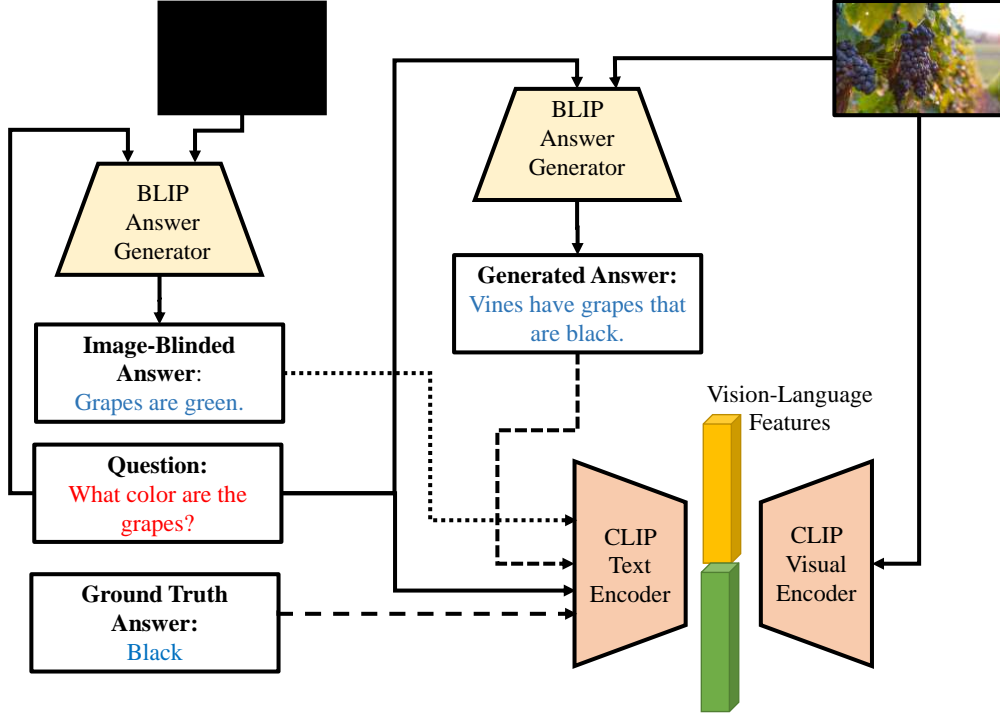


Figure 11: The architecture of CLIP-BLIP network as a baseline for PW-VQA. We combine generative pretrained BLIP Li et al. [2022] with encoding of the CLIP Radford et al. [2021] as a transformer-based large vision-language model.

Table 2: The table lists the accuracy values for different backbones based on VQA-CP v2 and VQA v2 datasets. We use different backbones, UpDn, S-MRL, and CLIP-BLIP, to show the effect of the backbone on the accuracy. We show the best-performing method with bold and the second-best-performing method with an underline.

Test set Methods	Base	VQA-CP v2 test				VQA v2 test			
		All	Y/N	Num.	Other	All	Y/N	Num.	Other
PW-VQA (ours)	UpDn	59.06	<u>88.26</u>	52.89	45.45	<u>62.63</u>	81.80	43.90	<u>53.01</u>
PW-VQA (ours)	S-MRL	60.26	88.09	<u>59.13</u>	45.99	61.25	80.32	43.17	51.53
PW-VQA (ours)	CLIP-BLIP	76.57	97.23	69.39	67.72	78.17	97.27	62.26	67.85

A.3 More Qualitative Examples

Qualitative comparison of VQA-CP v2 test split, our method vs. CF-VQA [Niu et al., 2021] and regular VQA are shown in Fig. 12. Red bars denote the ground-truth one, while the other bars denote the prediction probability corresponding to their value. As shown in this figure, all methods fail on the question and image pairs that require background knowledge and reasoning.

A.4 Stabilizing logarithmic computations

We noticed that adding a constant ϵ to the logarithmic computations of the fusion equations is important for the training and test consistency. For this reason, we also tried different ϵ to stabilize logarithmic computations of the loss function and include it in the ablation study. The results are reported in Tab. 3, and are shown in Fig. 13.

[t]

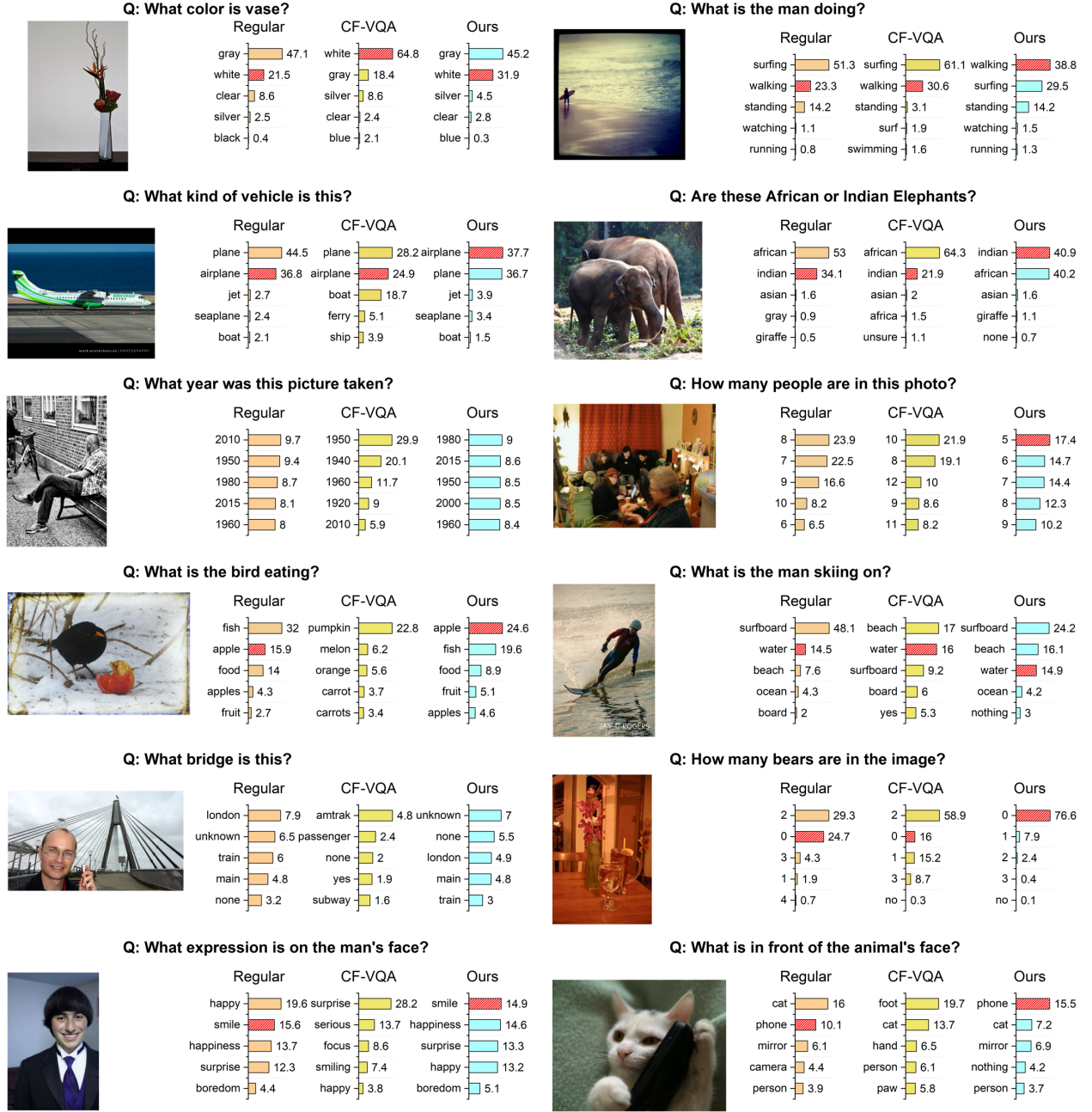


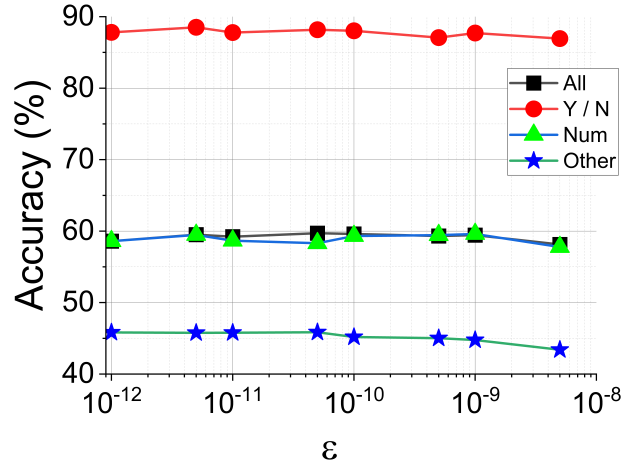
Figure 12: Qualitative comparison of VQA-CP v2 test split, our method vs. CF-VQA [Niu et al., 2021] and regular VQA are shown in these images. Red bars denote the ground-truth one, while the other bars denote the prediction probability corresponding to their value.

A.5 Categorized improvements on SAN, UpDn, and SMRL baselines

The plots in Fig. 14 show performance metrics for different methods as baseline and percent of improvements compared to baseline on each class of question types when using our proposed method, PW-VQA. In all of these simulations, $\alpha = 1.4$ are set. As seen in Fig. 14, PW-VQA consistently improves the existing method, confirming the generalizability of the method to several existing methods.

Table 3: Ablation of different values of ϵ on VQA-CP v2 test set. The backbone here is the SMRL network.

ϵ	All	Y / N	Num	Other
1.00E-12	58.6	87.81	58.59	45.82
5.00E-12	59.51	88.51	59.47	45.77
1.00E-11	59.22	87.78	58.66	45.79
5.00E-11	59.71	88.18	58.31	45.85
1.00E-10	59.6	88.03	59.32	45.19
5.00E-10	59.31	87.07	59.44	45.02
1.00E-09	59.44	87.71	59.6	44.77
5.00E-09	58.13	86.94	57.78	43.41

Figure 13: Ablation of different values of epsilon on VQA-CP v2 test set. Variations of ϵ has a slight effect on improving the results, though the reason may be related to computational stability. These results are related to PW-VQA with $\alpha = 1.5$ and $\epsilon = \{10^{-12}, 5 \times 10^{-12}, \dots, 5 \times 10^{-9}\}$.

A.6 Statistical analysis of performance values

Variances of the accuracy results and mean values of the method are listed in Tab. 4.

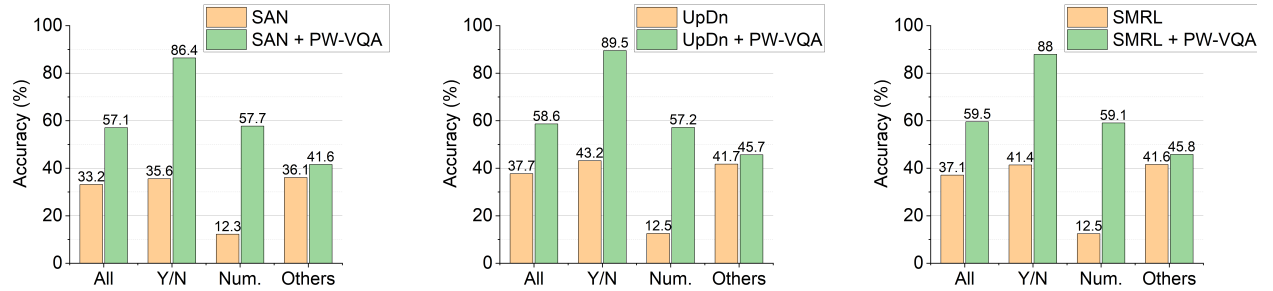
Figure 14: The plots here show the performance metrics in percent for different backbones using our proposed method, PW-VQA. All $\alpha = 1.4$ are set for all these simulations. Digits on the bars are rounded up to one digit. As shown here, the proposed method consistently improves the performance of all the backbone.

Table 4: Variances of the accuracy performance of our method based on five performing simulations with different random seeds.

Dataset	Base	Overall	Y/N	Num.	Other
VQA v2	S-MRL	60.76 \pm 0.10	79.60 \pm 0.47	42.75 \pm 0.07	51.21 \pm 0.03
VQA v2	UpDn	62.62 \pm 0.01	81.80 \pm 0.06	43.59 \pm 0.05	53.09 \pm 0.01
VQA-CP v2	S-MRL	59.71 \pm 0.14	87.98 \pm 0.24	59.41 \pm 0.61	45.51 \pm 0.09
VQA-CP v2	UpDn	58.70 \pm 0.20	89.19 \pm 0.23	58.85 \pm 0.56	45.17 \pm 0.05

Table 5: Ablation study on different backbones, namely SAN, S-MRL, and UpDn, as listed here. As listed, our proposed method is improving the results when used with all of the backbones here, and also improves as we use the fusion and causal graph that is proposed. The fusion function is with $\alpha = 1.4$ as the free parameter and based on empirical study.

	All	Y/N	Num.	Other
SAN [Yang et al., 2016]	32.77	38.12	12.38	35.56
SAN+EA	46.25	62.13	37.58	40.31
+PW-VQA (EA)	57.06	86.4	57.73	41.57
	All	Y/N	Num.	Other
UpDn [Anderson et al., 2018]	37.55	42.11	12.88	41.93
UpDn (EA)	47.02	65.89	18.11	45.06
+PW-VQA (EA)	58.64	89.51	57.15	45.68
	All	Y/N	Num.	Other
S-MRL Cadene et al. [2019a]	36.59	40.71	13.17	40.85
S-MRL (EA)	49.65	72.48	24.42	44.6
+PW-VQA (EA)	59.54	87.95	59.05	45.83

A.7 Causal graph improvements

Table 5 presents an ablation study on the effect of the backbone and how our causal graph and proposed method improve the results. These results are excluding the EA fusion strategy and therefore, are to study the effect of a solely causal counterfactual mechanism that is to block vision-fusion collider bias.

A.8 Effect of α variations on the performance

Ablation study of PW-VQA α values on the final performance result for α values ranging from 1 to 2 are listed in Tab. 6. As listed and seen in the table, the $\alpha = 1.4$ works well for most of the backbones.

Table 6: Ablation of PW-VQA α values on the final result for values ranging from 1 to 2. As shown the value of $\alpha = 1.4$ works well for most of the backbones.

	All	Y / N	Num	Other
SAN	33.18	38.57	12.25	36.1
$\alpha = 1$	56.23	86.2	57.72	40.3
$\alpha = 1.1$	56.27	87.45	58.5	39.54
$\alpha = 1.2$	56.96	86.84	58.07	41.57
$\alpha = 1.3$	52.9	76.87	57.67	39.95
$\alpha = 1.4$	57.06	86.4	57.73	41.57
$\alpha = 1.5$	42.75	51.24	52.24	39.38
$\alpha = 1.6$	55.1	85.64	58.31	38.39
$\alpha = 1.7$	56.2	86.41	58.21	41.15
$\alpha = 1.8$	53.85	87.36	54.65	39.3
$\alpha = 1.9$	43.41	73.47	57.52	34.49
$\alpha = 2$	53.39	86.22	52.64	39.26

	All	Y / N	Num	Other
UpDn	37.69	43.17	12.53	41.72
$\alpha = 1$	57.75	89.09	53.25	45.05
$\alpha = 1.1$	58.45	89.8	55.5	45.86
$\alpha = 1.2$	57.55	89.22	57.24	43.08
$\alpha = 1.3$	57.64	89.24	54.1	45.67
$\alpha = 1.4$	58.64	89.51	57.15	45.68
$\alpha = 1.5$	59.13	89.34	57.71	45.38
$\alpha = 1.6$	58.59	88.18	58.08	45.2
$\alpha = 1.7$	56.96	89.07	45.16	44.78
$\alpha = 1.8$	57.09	89.34	54.69	44.83
$\alpha = 1.9$	58.91	88.51	59.66	44.14
$\alpha = 2$	58.67	88.16	59.84	43.95

	All	Y / N	Num	Other
S-MRL	37.09	41.39	12.46	41.6
$\alpha = 1$	59.47	88.57	58.55	45.44
$\alpha = 1.1$	59.49	89.1	58.95	45.45
$\alpha = 1.2$	59.17	87.76	59.53	45.54
$\alpha = 1.3$	59.24	87.86	59.04	45.71
$\alpha = 1.4$	59.54	87.95	59.05	45.83
$\alpha = 1.5$	59.71	88.18	58.31	45.85
$\alpha = 1.6$	59.44	88.02	58.83	45.43
$\alpha = 1.7$	59.42	87.79	59.27	45.24
$\alpha = 1.8$	59.26	87.5	59.56	44.8
$\alpha = 1.9$	58.82	87.11	59.29	44.31
$\alpha = 2$	58.4	86.51	57.55	43.99